Article:

Muzikar, P. and Heaton, T.J. orcid.org/0000-0002-9994-142X (2022) Wiggle matching with correlations. Radiocarbon, 64 (1). pp. 187-194. ISSN 0033-8222

https://doi.org/10.1017/rdc.2021.106

Wiggle matching with correlations

Paul Muzikar
Department of Physics and Astronomy, Purdue University
West Lafayette, IN 47907
and
Timothy J. Heaton
School of Mathematics and Statistics, University of Sheffield
Sheffield S3 7RH, UK

August 10, 2021

Abstract

Wiggle matching is an important and powerful technique in radiocarbon dating that can be used to improve the precision of calendar age estimates. All radiocarbon determinations require calibration to provide calendar age estimates. This calibration is achieved by comparing the determinations against a calibration curve $\mu(\cdot)$ to calculate the probability the sample arises from any particular calendar age t. Wiggle matching involves the calibration of a set of radiocarbon determinations taken from samples with known separations between their calendar ages. Since the calendar age separations between samples are known, all the calendar ages are known functions of one particular age, T_1 — commonly the most recent calendar age. Dating the sequence then reduces to considering $p(T_1 = t_1|data)$, the probability of the calendar age t_1 given the set of radiocarbon determinations. In previous work, a Bayesian approach has been used to derive a nice formula for this quantity under the assumption we have independent pointwise estimates of the calibration curve $\mu(t)$. In this paper, we derive a generalization of this formula showing how to incorporate covariance information from the calibration curve under an assumption of multivariate normality.

Introduction

Wiggle matching is a powerful technique used in radiocarbon dating to improve the precision with which one can estimate calendar ages of samples (Pearson, 1986). The classic usage of the technique is when seeking to estimate the calendar ages of a series of tree-ring samples for which, due to ring counting, the number of calendar years separating the samples is known precisely. By calibrating multiple determinations jointly within a wiggle match we can improve the precision in our absolute calendar age estimates compared with the estimate we would obtain with just a single determination.

Suppose we are dating such a tree-ring sequence consisting of N determinations from consecutive annual rings, such that we know that the true, calendar ages must be $T_1, T_2 = T_1+1, T_3 = T_1+2, \ldots, T_N = T_1+N-1$. Given T_1, all the other ages are known and so this is the only unknown we need to estimate. We obtain radiocarbon data for each tree ring, and then try to match the ups and downs in the data to ups and downs in the calibration curve, knowing that we have N consecutive years.

Bayesian theory has been applied to make this method quantitative, (see for example, Christen and Litton, 1995; Bronk Ramsey et al., 2001). The net result is an expression, in terms of the data, for $p(T_1 = t_1|data)$, the probability for the unknown age T_1 given the set of N radiocarbon determinations. This expression is also dependent upon the value of the calibration curve $\mu(t_1), ..., \mu(t_1 + N - 1)$. The formulae given in these papers assume pointwise estimates of the calibration curve which are independent from one another and ignore any potential covariance information between the estimates at adjacent times.

The importance of such covariance structure in the calibration curve has long been understood, see for example Blackwell and Buck (2008) and Millard (2008). Millard (2008) discusses wiggle matching and covariance, and provides results of several wiggle matching calculations which incorporate the covariance information from the calibration curve.

Our goal in this brief note is to derive a generalization of the usual Bayesian wiggle-match formulation for $p(T_1 = t_1|data)$, to show how this result is modified by the covariance effects under the assumption that the calibration curve is modelled as a multivariate normal distribution. Our final answer, a new expression for $p(T_1 = t_1|data)$, is given by equations (8) - (10). It has the same general structure as the usual formula, and it explicitly shows how the covariance information from the calibration curve enters into the result. The next section contains our derivation. As much as possible, we use the approach and notation already developed for this type of analysis — for examples, see Heaton et al. (2009, 2020), Bronk Ramsey (2015), Niu et al. (2013), and Blackwell and Buck (2008).

Bayesian theory

We denote the true, unknown calendar ages of our N samples by $\{T_i\}_{i=1}^N$, and the observed radiocarbon determinations (either radiocarbon ages or $^{14}C/^{12}C$ ratios) by $\mathbf{y} = (y_1, \ldots, y_n)^T$. We denote the unknown true value of the calibration curve (either the true radiocarbon age or $^{14}C/^{12}C$ ratio for calendar age t cal BP) in any calendar year by $\mu(t)$. Thus, we have

$$p(y_i|T_i = t_i, \mu(t_i)) = \frac{1}{\sqrt{2\pi\sigma_i^2}} \exp(-\frac{(y_i - \mu(t_i))^2}{2\sigma_i^2}), \tag{1}$$

where σ_i is the uncertainty in the radiocarbon measurement. We do not know the true value of the calibration curve (i.e., the true value of radiocarbon age or ${}^{14}C/{}^{12}C$ ratio corresponding to calendar age t cal BP) but we do have pointwise estimates $\hat{\mu}(t)$ in any given year, so that we have

$$\mu(t) = \hat{\mu}(t) + \epsilon(t). \tag{2}$$

The $\epsilon(t)$ denotes our uncertainty in the calibration curve at time t. Typically there will be covariance in these values — $\epsilon(t)$ will not be independent of $\epsilon(t+1)$. If we assume that these uncertainties have a multivariate Gaussian form and consider any sequence of N consecutive calendar years $\mathbf{t} = (t, t+1, \ldots, t+N-1)^T$:

$$p(\boldsymbol{\epsilon}_t) = (2\pi)^{-N/2} \det(\boldsymbol{\Sigma}_t)^{-\frac{1}{2}} \exp\left(-\frac{1}{2}\boldsymbol{\epsilon}_t^T \boldsymbol{\Sigma}_t^{-1} \boldsymbol{\epsilon_t}\right), \tag{3}$$

where $\boldsymbol{\epsilon}_t = (\epsilon(t), \ldots, \epsilon(t+N-1))^T$ and $\boldsymbol{\Sigma}_t$ is the covariance matrix which encodes the correlations in the $\boldsymbol{\epsilon}_t$ uncertainties, and in general will depend on t. According to equation (2), for any vector of calendar ages $\mathbf{t}$, we have $\boldsymbol{\mu}_t = \hat{\boldsymbol{\mu}}_t + \boldsymbol{\epsilon}_t$. Here $\boldsymbol{\mu}_t$ denotes the vector of true radiocarbon ages or ${}^{14}C/{}^{12}C$ ratios (to correspond to choice of the y_i's) for the sequence of calendar age $\mathbf{t}$, and $\hat{\boldsymbol{\mu}}_t$ the corresponding pointwise estimates.

We are now ready to begin our derivation. We first note that the quantity we want is $f(t_1) = p(T_1 = t_1|data) = p(T_1 = t_1|\mathbf{y})$. To calculate this we use Bayes' Theorem:

$$f(t_1) = p(T_1 = t_1|data) = p(T_1 = t_1|\mathbf{y}) = ap(\mathbf{y}|t_1)\pi_0(t_1) \tag{4}$$

Here, a is a normalization constant, and $\pi_0(t_1)$ is the prior probability for T_1. We expand $p(\mathbf{y}|t_1)$ to obtain (to save writing, we denote $t_j = t_1 + j - 1$, the calendar age of the j^{th} determination in the sequence to be wiggle-matched)

$$\begin{aligned} f(t_1) = a \int \ldots \int \Bigg[\Bigg\{ \prod_{j=1}^{N} \int p(y_j|t_1, \mu(t_j)) p(\mu(t_j)|t_1, \epsilon(t_j))\, d\mu(t_j) \Bigg\} \\ \times\, p(\epsilon(t_1), \ldots, \epsilon(t_N)|t_1)\pi_0(t_1) \Bigg] d\epsilon(t_1) \ldots d\epsilon(t_N), \end{aligned} \tag{5}$$

We note that $p(\mu(t_j)|t_1, \epsilon(t_j)) = \delta(\mu(t_j) - \hat{\mu}(t_j) - \epsilon(t_j))$, where $\delta()$ is the Dirac delta function. Thus we have

$$\begin{aligned} f(t_1) = a \int \ldots \int \Bigg[\Bigg\{ \prod_{j=1}^{N} \int \exp\left(-\frac{(y_j - \mu(t_j))^2}{2\sigma_j^2}\right) \delta(\mu(t_j) - \hat{\mu}(t_j) - \epsilon(t_j))\, d\mu(t_j) \Bigg\} \\ \times\, p(\epsilon(t_1), \ldots, \epsilon(t_N)|t_1)\pi_0(t_1) \Bigg] d\epsilon(t_1) \ldots d\epsilon(t_N). \end{aligned} \tag{6}$$

Note that we keep absorbing into the normalization constant a those factors that do not depend on t_1. Doing the integral over $\mu(t_1), \ldots, \mu(t_N)$ gives

$$\begin{aligned} f(t_1) = a \int \ldots \int \Bigg[\exp\left(-\sum_{j=1}^{N} \frac{(y_j - \hat{\mu}(t_j) - \epsilon(t_j))^2}{2\sigma_j^2}\right) \\ \times \det(\boldsymbol{\Sigma}_{t_1})^{-\frac{1}{2}} \exp\left(-\frac{1}{2}\boldsymbol{\epsilon}_t^T \boldsymbol{\Sigma}_t^{-1} \boldsymbol{\epsilon}_t\right) \pi_0(t_1) \Bigg] d\epsilon(t_1) \ldots d\epsilon(t_N). \end{aligned} \tag{7}$$

Finally, we do the integral over the $\epsilon(t_1), \ldots, \epsilon(t_N)$ to get

$$f(t_1) = a\sqrt{\frac{\det(\boldsymbol{\Sigma}_{t_1}^{-1})}{\det(\boldsymbol{T}_{t_1})}}\exp(-\frac{1}{2}(\hat{\boldsymbol{\mu}}_{t_1} - \mathbf{y})^T \boldsymbol{W}_{t_1}(\hat{\boldsymbol{\mu}}_{t_1} - \mathbf{y}))\pi_0(t_1). \tag{8}$$

This is our final answer; it is similar to usual Bayesian result in being a multivariate Gaussian in $\hat{\boldsymbol{\mu}}_{t_1} - \mathbf{y}$. However, it now involves the $N \times N$ matrix $\boldsymbol{W}_{t_1}$, which in general has off-diagonal terms. This matrix is given by

$$[W_{t_1}]_{ij} = \frac{1}{\sigma_i^2}\delta_{ij} - \frac{1}{\sigma_i^2\sigma_j^2}\left[T_{t_1}^{-1}\right]_{ij} \qquad [T_{t_1}]_{ij} = \left[\Sigma_{t_1}^{-1}\right]_{ij} + \frac{1}{\sigma_i^2}\delta_{ij}. \tag{9}$$

In general these matrices, as well as the determinants of $\boldsymbol{\Sigma}_{t_1}^{-1}$ and $\boldsymbol{T}_{t_1}$, will depend on t_1.

The matrix $\boldsymbol{W}_{t_1}$ can be written in a more compact, elegant form. If we define a diagonal matrix $D_{ij} = \sigma_i^2\delta_{ij}$, containing the variances of the radiocarbon determinations $\mathbf{y}$ on the diagonal, then we may write

$$\boldsymbol{W}_{t_1} = (\boldsymbol{D} + \boldsymbol{\Sigma}_{t_1})^{-1}. \tag{10}$$

To derive this, we can go back to equation (4), and evaluate $p(\mathbf{y}|t_1)$ in the following way. We note that the N-dimensional random variable $\mathbf{y} - \hat{\boldsymbol{\mu}}_{t_1}$ can be viewed as the sum of two, independent, multivariate Gaussians, each with a mean of zero, and with covariance matrices given by $\boldsymbol{\Sigma}_{t_1}$ and by $\boldsymbol{D}$. It is well known that the probability density of this sum is itself a Gaussian, with a covariance matrix given by $\boldsymbol{D} + \boldsymbol{\Sigma}_{t_1}$. The equivalence of these two forms for $\boldsymbol{W}_{t_1}$, given in equations (9) and (10), is shown in the Appendix.

Special Cases

Certain special cases are instructive. First, suppose that there are no correlations among the $\epsilon(t_j)$. This implies that $\boldsymbol{\Sigma}$ is a diagonal matrix:

$$\Sigma_{ij} = s_j^2\delta_{ij} \tag{11}$$

Thus, s_j^2 is the variance in the calibration curve at time t_j. It is then straightforward to show that the $\boldsymbol{W}$ matrix becomes

$$W_{ij} = \frac{1}{\sigma_j^2 + s_j^2}\delta_{ij} \tag{12}$$

This is the usual Bayesian result (Christen and Litton, 1995; Bronk Ramsey et al., 2001), which we recover for this case; any differences in $\boldsymbol{W}$ from this usual result thus are totally due to correlations among the $\epsilon(t_j)$.

Another special case to consider is if the radiocarbon determinations are very precise, so that all of our uncertainty comes from the calibration curve, Taking $\sigma_j \to 0$ then gives $\boldsymbol{W} = \boldsymbol{\Sigma}_t^{-1}$. The Gaussian in the wiggle matching formula (8) then directly reflects the covariance matrix from the calibration curve.

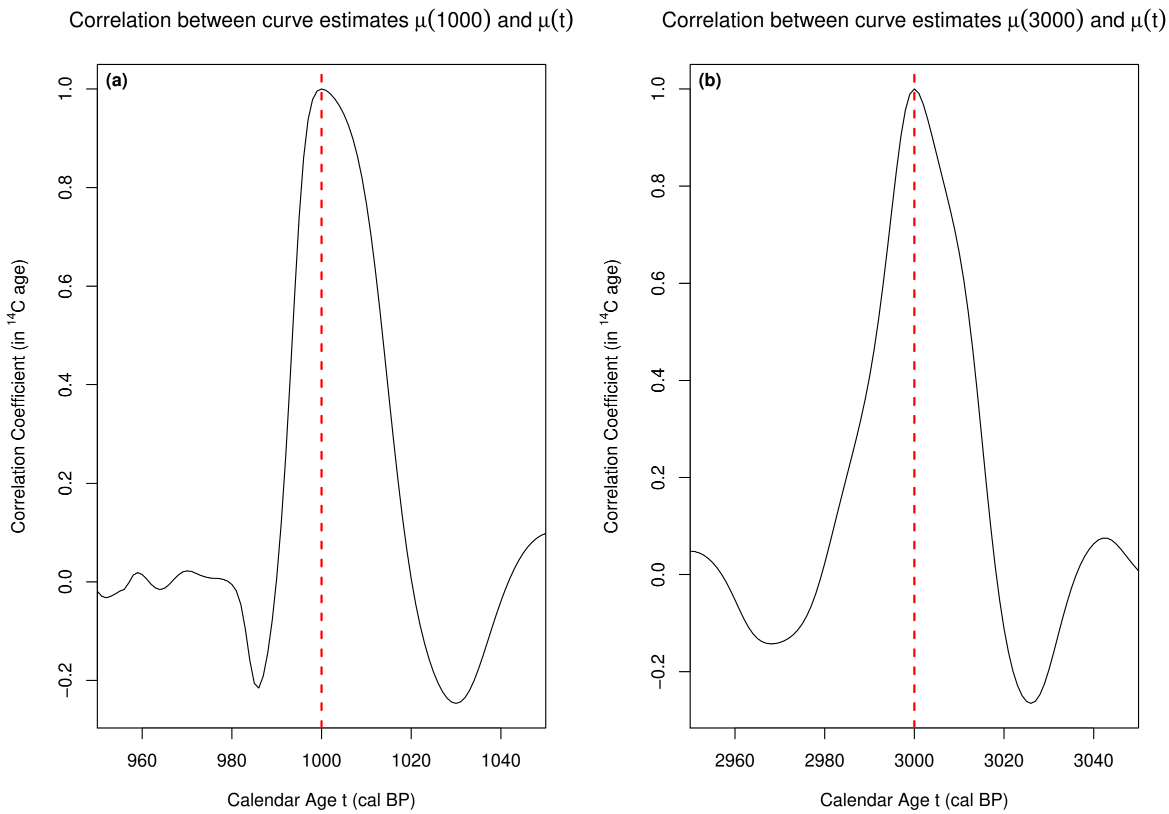

Figure 1: An illustration of the correlation in the IntCal20 calibration curve. Panel a) shows the correlation between the value of the calibration curve at 1000 cal BP, i.e. $\mu(1000)$*, and* $\mu(t)$ *for* $950 \leq t \leq 1050$ *(50 calendar years either side). Panel b) the correlation between* $\mu(3000)$ *and* $\mu(t)$*, for* $2950 \leq t \leq 3050$*. The quantity plotted on the y-axis is given by equation (15).*

Role of the covariance matrix Σ

It is perhaps not easy to understand the role played in the wiggle matching equation by the off-diagonal elements of the covariance matrix Σ_{ij}; these would be $\mathrm{Cov}(\epsilon(t_i), \epsilon(t_j))$ for $i \neq j$. To gain some insight, we can consider the following special case: suppose that the off-diagonal elements of Σ are much smaller than the diagonal elements. Thus we write

$$\Sigma_{ij} = s_i^2 \delta_{ij} + G_{ij} \tag{13}$$

where $G_{ij} = 0$ for $i \neq j$. If we now assume that the elements of G are small compared to the diagonal elements, we can derive the following result: to first order in G we have

$$W_{ij} \approx \frac{1}{\sigma_j^2 + s_j^2}\delta_{ij} - \frac{G_{ij}}{(\sigma_i^2 + s_i^2)(\sigma_j^2 + s_j^2)} \tag{14}$$

The effect of the diagonal first term is clear: when inserted into equation (8) it will assign higher probabilities to values of t_1 which make the magnitudes of the various $y_i - \mu(t_i)$ as small as possible. The second, off-diagonal term will favor values of t_1 which cause the various products $(y_i - \hat{\mu}(t_i))(y_j - \hat{\mu}(t_j))$ to have the same sign as G_{ij}. Thus, if, for example, G_{23} is positive, the off-diagonal term will favor values of t_1 which make $(y_2 - \hat{\mu}(t_2))(y_3 - \hat{\mu}(t_3))$ positive.

To give some sense of how large the off-diagonal terms can be, we present examples of the correlations in the IntCal20 curve, and how they decay as the distance between calendar ages increases. In Figure 1 we plot the correlation between $\mu(t)$ and $\mu(t^\star)$ for $t^\star = 1000$, and for $t^\star = 3000$ cal BP. In terms of our present notation, the correlation function $C(t, t^\star)$ plotted is given by

$$C(t, t^\star) = \frac{< \epsilon(t)\epsilon(t^\star) >}{\sqrt{< \epsilon^2(t) >< \epsilon^2(t^\star) >}} \tag{15}$$

where the brackets indicate the expectation over the random variables $\epsilon(t)$.

We see that the off-diagonal terms are comparable to the diagonal ones over about 10 - 20 years in both cases; thus, over the range of a short wiggle-match (ca. 20 calendar years), correlations can be significant.

Discussion

We have discussed a generalization of the usual Bayesian approach to wiggle matching. The key ingredients in this formulation are the pointwise mean estimates of the calibration curve $\hat{\mu}(t)$, and the corresponding curve covariance which for any set of N consecutive years we assume can be encoded in an $N \times N$ covariance matrix $\mathbf{\Sigma}$. As we have shown, information about these quantities can be provided by the constructors of the calibration curve; for relevant discussion of the newly presented calibration curves, see, for example Heaton et al. (2020), Reimer et al. (2020) and van der Plicht et al. (2020).

The ultimate origins of the correlated uncertainties in the calibration curve (the off-diagonal elements of Σ_{ij}) should perhaps be discussed. When constructing the radiocarbon calibration curve, we assume that the underlying curve $\mu(t)$ one is trying to estimate is somewhat smooth, i.e., that the level of ^{14}C in the atmosphere in calendar year t is similar to that in year $t + 1$. This is the basis of most statistical regression techniques and means that information on the value of the curve in one calendar year also informs you about what its value is likely to be in neighbouring years. Indeed, it is this assumption of smoothness which allows you to borrow and combine information from multiple ^{14}C observations over a neighbourhood to strengthen the curve estimate in any individual year and prevent overfitting to the data. Without it, you could make no prediction about the value in a calendar year in which you did not have a direct observation.

This smoothness creates a level of dependence in the resultant curve estimate that provides more information than, and goes beyond, just the pointwise intervals for $\hat{\mu(t)}$. It is unlikely that the true atmospheric ^{14}C levels will flip from the top of the curve's probability interval to the bottom in the space of a single year. Rather if the true value of the curve lies towards the top (bottom) of the probability interval in year t, it is likely to also lie towards the top (bottom) of the interval in nearby times t'. In our notation, $\epsilon(t)$ and $\epsilon(t')$ are likely to have the same sign when t' is in the neighbourhood of t.

The level of smoothness, and hence dependence, in the calibration curve will be affected by the nature of the reference ^{14}C data used to construct the calibration curve (to which we aim to adapt) and, in the case of IntCal20, the number and placement of the knots in the underlying spline. Over time spans with a lower density of knots, the resulting estimate for the calibration curve will however be smoother, and this will tend to create longer lasting curve covariance. There are also specific times, during solar proton (SPE or Miyake) type events, where the smoothness of the IntCal curve is permitted to be reduced.

The diverse nature of the ^{14}C data used to construct the IntCal curve will also influence the covariance in the final calibration curve estimate. In particular, in the older portion of the calibration curve ($> 14,000$ cal yr BP) where the calendar ages and ^{14}C measurements of the reference data themselves exhibit significant covariance. Here the calibration curve is informed by ^{14}C measurements from floating tree-ring sequences (Adolphi et al., 2017; Turney et al., 2010, 2016) for which the internal chronologies are known, but the absolute ages are not — these are adaptively wiggle-matched, during curve construction, to fit with the rest of the reference ^{14}C data. The calendar ages of the macrofossils from Lake Suigetsu (Bronk Ramsey et al., 2020) also possess covariance, as do the foraminifera from ocean sediments (Bard et al., 2013; Hughen and Heaton, 2020) which are linked to the Hulu Cave timescale by the tying of global abrupt palaeoclimatic events (Heaton et al., 2013). The speleothem ^{14}C measurements (e.g., Cheng et al., 2018; Southon et al., 2012) share a common dead carbon fraction; and the marine based ^{14}C measurements (e.g., Bard et al., 2013; Hughen and Heaton, 2020) also share a ^{14}C offset due to the modelling of the marine reservoir age (Butzin et al., 2020). All these covariances within the constituent IntCal reference data will affect, and tend to increase, the covariance on the final curve estimate $\hat{\mu})(t)$ in this time period, see Heaton et al. (2020) for details.

Acknowledgements

This work was supported by National Science Foundation grant EAR 0112480 and a Leverhulme Trust Fellowship RF-2019-140\9 .

Appendix

We want to prove that the two expressions (9) and (10) given for the matrix W are equivalent. The normalising constant obtained in (8) can also be shown to be equivalent to the approach using the result that the sum of two multivariate Gaussians is Gaussian, although we do not show this here. In this Appendix, all the symbols represent $N \times N$ matrices, so we omit the bold face notation. The two forms are:

$$W_A = D^{-1} - D^{-1}(\Sigma^{-1} + D^{-1})^{-1}D^{-1} \qquad W_B = (D + \Sigma)^{-1} \tag{16}$$

where D and Σ are defined in the main text. W_A is the form given by equation (9), while W_B is the form given by equation (10). It is sufficient to show that $W_B^{-1}W_A = I$, where I is the identity matrix. One useful relation is that for two matrices, $(HY)^{-1} = Y^{-1}H^{-1}$. Thus

$$D^{-1} + \Sigma^{-1} = D^{-1}(I + D\Sigma^{-1}) \qquad (D^{-1} + \Sigma^{-1})^{-1} = (I + D\Sigma^{-1})^{-1}D \tag{17}$$

So we evaluate

$$W_B^{-1}W_A = (D + \Sigma)(D^{-1} - D^{-1}(\Sigma^{-1} + D^{-1})^{-1}D^{-1}) \tag{18}$$

or

$$W_B^{-1}W_A = I + \Sigma D^{-1} - (I + D\Sigma^{-1})^{-1} - \Sigma D^{-1}(I + D\Sigma^{-1})^{-1} \tag{19}$$

or

$$W_B^{-1}W_A = I + K - (I + K)(I + K^{-1})^{-1} \tag{20}$$

where $K = \Sigma D^{-1}$. Note that

$$I + K^{-1} = K^{-1}(I + K) \qquad (I + K^{-1})^{-1} = (I + K)^{-1}K \tag{21}$$

Finally we have

$$W_B^{-1}W_A = I + K - (I + K)(I + K)^{-1}K = I \tag{22}$$

References

Adolphi, F., Muscheler, R., Friedrich, M., Güttler, D., Wacker, L., Talamo, S., and Kromer, B. (2017). Radiocarbon calibration uncertainties during the last deglaciation: Insights from new floating tree-ring chronologies. *Quaternary Science Reviews*, 170:98–108.

Bard, E., Ménot, G., Rostek, F., Licari, L., Böning, P., Edwards, R., Cheng, H., Wang, Y., and Heaton, T. (2013). Radiocarbon calibration/comparison records based on marine sediments from the Pakistan and Iberian margins. *Radiocarbon*, 55(4).

Blackwell, P. G. and Buck, C. E. (2008). Estimating radiocarbon calibration curves. *Bayesian Analysis*, 3(2):225 – 248.

Bronk Ramsey, C. (2015). *Mathematics and Archaeology*, chapter Bayesian approaches to the building of Archaeological Chronologies, pages 272–292. Taylor and Francis.

Bronk Ramsey, C., Heaton, T. J., Schlolaut, G., Staff, R. A., Bryant, C. L., Brauer, A., Lamb, H. F., Marshall, M. H., and Nakagawa, T. (2020). Reanalysis of the Atmospheric Radiocarbon Calibration Record from Lake Suigetsu, Japan. *Radiocarbon*, 62(4):989–999.

Bronk Ramsey, C., van der Plicht, J., and Weninger, B. (2001). 'Wiggle Matching' Radiocarbon Dates. *Radiocarbon*, 43(2A):381–389.

Butzin, M., Heaton, T. J., Köhler, P., and Lohmann, G. (2020). A Short Note on Marine Reservoir Age Simulations Used in IntCal20. *Radiocarbon*, 62(4):865–871.

Cheng, H., Lawrence Edwards, R., Southon, J., Matsumoto, K., Feinberg, J. M., Sinha, A., Zhou, W., Li, H., Li, X., Xu, Y., Chen, S., Tan, M., Wang, Q., Wang, Y., and Ning, Y. (2018). Atmospheric $^{14}C/^{12}C$ changes during the last glacial period from Hulu Cave. *Science*, 362(6420):1293–1297.

Christen, J. and Litton, C. (1995). A Bayesian approach to wiggle-matching. *Journal of Archaeological Science*, 22(6):719–725.

Heaton, T., Bard, E., and Hughen, K. (2013). Elastic tie-pointing-transferring chronologies between records via a Gaussian process. *Radiocarbon*, 55(4).

Heaton, T. J., Blaauw, M., Blackwell, P. G., Bronk Ramsey, C., Reimer, P. J., and Scott, E. M. (2020). The IntCal20 Approach to Radiocarbon Calibration Curve Construction: A New Methodology Using Bayesian Splines and Errors-in-Variables. *Radiocarbon*, 62(4):821—-863.

Heaton, T. J., Blackwell, P. G., and Buck, C. E. (2009). A Bayesian Approach to the Estimation of Radiocarbon Calibration Curves: The IntCal09 Methodology. *Radiocarbon*, 51(4):1151–1164.

Hughen, K. and Heaton, T. (2020). Updated Cariaco Basin ^{14}C Calibration Dataset from 0-60 cal kyr BP. *Radiocarbon*, 62(4).

Millard, A. R. (2008). Comment on "Estimating radiocarbon calibration curves". *Bayesian Analysis*, 3(2):255–262.

Niu, M., Heaton, T. J., Blackwell, P. G., and Buck, C. E. (2013). The Bayesian Approach to Radiocarbon Calibration Curve Estimation: The IntCal13, Marine13, and SHCal13 Methodologies. *Radiocarbon*, 55(4):1905–1922.

Pearson, G. W. (1986). Precise Calendrical Dating of Known Growth-Period Samples Using a 'Curve Fitting' Technique. *Radiocarbon*, 28(2A):292–299.

Reimer, P. J., Austin, W. E. N., Bard, E., Bayliss, A., Blackwell, P. G., Bronk Ramsey, C., Butzin, M., Cheng, H., Edwards, R. L., Friedrich, M., Grootes, P. M., Guilderson, T. P., Hajdas, I., Heaton, T. J., Hogg, A. G., Hughen, K. A., Kromer, B., Manning, S. W., Muscheler, R., Palmer, J. G., Pearson, C., van der Plicht, H., Reimer, R. W., Richards, D. A., Scott, E. M., Southon, J. R., Turney, C. S. M., Wacker, L., Adolphi, F., Büntgen, U., Capano, M., Fahrni, S., Fogtmann-Schulz, A., Friedrich, R., Köhler, P., Kudsk, S., Miyake, F., Olsen, J., Reinig, F., Sakamoto, M., Sookdeo, A., and Talamo, S. (2020). The IntCal20 Northern Hemisphere radiocarbon age calibration curve (0–55 cal kBP). *Radiocarbon*, 62(4):725–757.

Southon, J., Noronha, A. L., Cheng, H., Edwards, R. L., and Wang, Y. (2012). A high-resolution record of atmospheric ^{14}C based on Hulu Cave speleothem H82. *Quaternary Science Reviews*, 33:32–41.

Turney, C. S. M., Fifield, L. K., Hogg, A. G., Palmer, J. G., Hughen, K., Baillie, M. G. L., Galbraith, R., Ogden, J., Lorrey, A., Tims, S. G., and Jones, R. T. (2010). The potential of New Zealand kauri (Agathis australis) for testing the synchronicity of abrupt climate change during the Last Glacial Interval (60,000–11,700 years ago). *Quaternary Science Reviews*, 29(27):3677–3682.

Turney, C. S. M., Palmer, J., Bronk Ramsey, C., Adolphi, F., Muscheler, R., Hughen, K. A., Staff, R. A., Jones, R. T., Thomas, Z. A., Fogwill, C. J., and Hogg, A. (2016). High-precision dating and correlation of ice, marine and terrestrial sequences spanning Heinrich Event 3: Testing mechanisms of interhemispheric change using New Zealand ancient kauri (Agathis australis). *Quaternary Science Reviews*, 137:126–134.

van der Plicht, J., Bronk Ramsey, C., Heaton, T. J., Scott, E. M., and Talamo, S. (2020). Recent Developments In Calibration For Archaeological And Environmental Samples. *Radiocarbon*, 62(4):1095–1117.